A Computational Method for Eu's Generalized Hydrodynamic Equations of Rarefied and Microscale Gasdynamics

R. S. Myong
Division of Aerospace and Mechanical Engineering
Gyeongsang National University
Chinju, Gyeongnam 660-701, South Korea
E-mail: *myong@nongae.gsnu.ac.kr*
and
Institute for Mathematics and its Applications
University of Minnesota
400 Lind Hall
207 Church Street S.E.
Minneapolis, MN 55455, USA

Subject classification: 65M06, 76N15, 76K05.

Key words: Rarefied and microscale gasdynamics, generalized hydrodynamic equations, finite volume method.

Submitted to **Journal of Computational Physics** on February 16, 2000.

Typed by *LaTeX*

Proposed Running Head:

Computational Method for Eu's Generalized Hydrodynamics.

Mail all correspondences to:

Rho Shin Myong
Division of Aerospace and Mechanical Engineering
Gyeongsang National University
Chinju, Gyeongnam 660-701, South Korea

Phone: 82-591-751-6107
Fax: 82-591-757-5622
E-mail: *myong@nongae.gsnu.ac.kr*

A Computational Method for Eu's Generalized Hydrodynamic Equations of Rarefied and Microscale Gasdynamics

R. S. Myong
Division of Aerospace and Mechanical Engineering
Gyeongsang National University
Chinju, Gyeongnam 660-701, South Korea*
E-mail: *myong@nongae.gsnu.ac.kr*
and
Institute for Mathematics and its Applications
University of Minnesota
400 Lind Hall
207 Church Street S.E.
Minneapolis, MN 55455, USA

Abstract

A computational method for solving Eu's generalized hydrodynamic equations, which have been recently proposed for modeling the motion of gases in non-equilibrium state by Eu (*Kinetic Theory and Irreversible Thermodynamics*, 1992) and studied extensively by Myong(*Physics of Fluids* 11-2, p. 2788, 1999) is presented. It has been shown that the new equations apply in all Mach numbers and satisfy the second law of thermodynamics at all Knudsen numbers and to every order of approximation. The computational method for the thermodynamically consistent Eu's generalized hydrodynamic equations is based on the finite volume formulation and exactly the same as the Navier-Stokes codes, except for an additional routine of calculating shear stress and heat flux from the given conserved variables and thermodynamic forces. The method is tested for one-dimensional shock structure and two-dimensional flat plate flow problems to check its validity and potential. The numerical results indicate that the new computational model is efficient in calculating the high-Knudsen-number gas flow.

* All correspondences should be sent to this permanent address.

1 Introduction

Hypersonic vehicles at a high flight altitude experience various flow regimes; continuum, slip, transitional, and free-molecular. Owing to the low-density, the considerable parts of gas flows become high non-equilibrium [16]. Similar situation, from the different origin (small scale of the characteristic length), can be found in microscale gas flows, for example, internal flows in channels of microelectromechanical system (MEMS) [2, 15]. In consequence of high thermal non-equilibrium, new analysis tools beyond the Navier-Stokes equations based on the small deviation from local equilibrium are necessary.

Much efforts have been put into the development of such computational methods using hydrodynamic and kinetic approaches. One of the most successful method is the so-called direct simulation Monte Carlo (DSMC) method [5, 26] and it has been widely used to investigate hypersonic rarefied gas flows. However, the computational cost is very high in regimes near the continuum limit since it is based on tracking a large number of statistically representative particles. To reduce the computational cost, hybrid methods which couple an Euler or Navier-Stokes solver with DSMC were proposed [27]. Even though these approach can provide some benefits, there exist non-trivial issues for successful implementation of such approach: (1) when to switch between two different methods (continuum and kinetic); and (2) how to pass information from one method to another.

On the other hand, the hydrodynamic approach provides computationally efficient methods, for example, the Burnett equations [11], the Grad's moment equations [13], the BGK-Burnett equations [3], the moment equations based on the Gaussian moment closure [6, 19, 20], and the moment equations derived by the so-called extended thermodynamics [23]. However, it has been known that most of equations have difficulty in ensuring that the

second law of thermodynamics–one of natural laws–is satisfied for all conditions. [1] This problem can be manifested when either the shock-structure problem at a very high Mach number or the slip flow near the wall surface are considered. Of course, one may argue that it is only necessary to be consistent with the second law within the applicability range. In other words, it does not matter whether the second law is satisfied in regime beyond the applicability range or not since such regime is out of our interest. This argument is, however, misleading in the following sense: (1) it is very hard to know the exact range of applicability unless one actually solves the equations and compares with the Boltzmann solutions; (2) from a practical point of view not knowing the source of numerical troubles–whether it is caused by the violation of the basic physical laws or simply by numerical problems–can cause more troubles; and (3) the argument can preclude the possible benefit of satisfying the second law–for example, it works within applicability regime and is applicable even in the regime beyond, which is indeed the case with the Navier-Stokes equations.

On the ground of these points, we are led to take an alternative and yet unknown method such that the second law of thermodynamics is satisfied to every order of approximation or by whatever approximation made to the distribution function. This means that a formal mathematical structure of the entropy of irreversible processes in non-equilibrium state is developed and non-negative nature of the entropy production is rigorously proven. This new thermodynamically consistent hydrodynamic approach has been developed by Eu [10]. It is unique approach in the sense that the role of the entropy is taken into account at all steps of formulating the hydrodynamic equations from the Boltzmann equations. The motivation is that the most important role of higher-order terms is to increase the entropy, so that the second law of thermodynamics must be considered in all approximations. From

[1] For example, refer to papers [3, 7]. It is safe to say that the entropy production of the Burnett-type equations is not proved to be positive for all Knudsen numbers and flow conditions.

this line of reasoning, Eu found the non-equilibrium canonical distribution function and the cumulant expansion of the collision integral that can replace the so-called BGK linear approximation, which are believed to be new. It turned out that the new equations possess an unusual feature that the two extreme regimes of density–rarefied and dense–are covered, in other words, that both free-molecular and continuum limits are recovered.

The main problem in Eu's generalized hydrodynamics is that there exists a severe limitation in using it as a computational tool for the simulation of gas flows in multi-dimension. The difficulty comes from the complicated form of the constitutive relations by the existence of highly nonlinear terms. In the previous work [25], the nature of computational difficulty residing in Eu's generalized hydrodynamics was discussed. From the general understanding of the constitutive relations, an idea to overcome the difficulty of multi-dimensional extension has been proposed. The present work is intended to develop an efficient multi-dimensional computational method for Eu's generalized hydrodynamic equations on the basis of such idea.

The main feature of the present computational method can be summarized as follows. First, it is based on the hydrodynamic equations, which are proven to be consistent with macroscopic irreversible thermodynamics and at the same time are not restricted by the small Knudsen number assumption. In theory, it should be valid for all Knudsen numbers and under any flow condition. Second, the mathematical system of equations, like the Navier-Stokes equations, is of parabolic type. One may of course use the hyperbolic type, which is extensively studied in extended thermodynamics [23], since the hyperbolic system has some good mathematical properties. In this study, however, this approach is not used, simply because it is very hard to find any preferential direction of propagation in high-order moments (shear stress and heat flux), contrary to the case with conserved variables,

whose evolution must be restricted by the hyperbolic conservation laws. Lastly, besides the type of mathematical equation, the new method is designed to resemble the Navier-Stokes codes in every possible ways. The reason for this is that computational codes based on the Navier-Stokes equations turn out to be very robust and efficient. Many previous studies have indicated that, except for certain extreme conditions, the Navier-Stokes equations remain surprisingly robust [17]. For example, in rarefied Poiseuille flows, the velocity field predicted from the slip-corrected Navier-Stokes equations is in quantitative agreement with particle simulations. In addition, they are one of the most-studied mathematical equations, so that most of previous important results can go over to the present method.

2 Mathematical Models for Rarefied and Microscale Gas Transport

In nonlinear regime or processes occurring far from thermal equilibrium, for example, in rarefied and microscale gas transport, the mean free path becomes comparable with the characteristic length of the system. As a result, the linear fluid dynamic approximation (Navier-Stokes equations) breaks down and mathematical models in which the microscopic molecular nature of gas is taken fully into account must be used. These models range from fundamental equations of molecular interactions of particles–either deterministic (equation of motion solved by molecular dynamics method) or probabilistic (Klimontovich equation, and Liouville equation solved by Monte Carlo method)–to the Boltzmann equation, the DSMC solutions, and the high-order fluid dynamic equations. In principle, the fluid dynamic equations should be derived from the solution for the Boltzmann equation that yields a theory of macroscopic processes compatible with thermodynamics.

Mathematical models and solution methods for the description of the motion of gases are

summarized in Fig. 1. Only generalized hydrodynamic equations are retained since other fluid dynamic equations play a similar role. It must be, however, mentioned that most of other equations are not completely consistent with the second law of thermodynamics. From Fig. 1, it can be easily seen that the Boltzmann equation plays a central role in the hierarchy of mathematical models. It was derived by considering the collision dynamics of two particles and combining it with a statistical assumption in the form of the molecular chaos. Since the molecular chaos assumption is not of a mechanical nature, it should be regarded as a fundamental equation at the mesoscopic level of description of macroscopic processes in a dilute gas. The Boltzmann equation is a first-order differential equation in space and time, but its solution becomes very complicated because its integration is nonlinear due to the collisional integral. As a result, there can be an infinite variety of solutions. This means that given the Boltzmann equation as the kinetic equation the thermodynamics on the evolution of macroscopic variables are necessary to obtain the phenomenologically correct solution.

On the other hand, DSMC is fundamentally different from solution methods of the Boltzmann equation in the sense that it is not based on any mathematical equations, but simulates directly the particles' motion and interaction. Conceptually, it starts from the Liouville equation and tracks a large number of statistically representative particles. Since this process corresponds to the introduction of molecular chaos assumption, it is generally believed that DSMC is equivalent to solving the Boltzmann equation for a monatomic gas undergoing binary collisions.

The derivation of fluid dynamic equations from the Boltzmann equation begins with a realization that there exist three collisional invariants in the Boltzmann equation: mass, total momentum, and energy. These are nothing but the hyperbolic conservation laws which

can also be derived from the point of view of continuum mechanics. The only problem is how to derive equations of high-order terms, namely, shear stress and heat flux. There are two methods for this problem: the Chapman-Enskog method, and the moment method. In the Chapman-Enskog method, the equations of high-order terms are derived by expanding the distribution functions in series of Knudsen number and by substituting them into the Boltzmann equation. In the moment method, they are obtained by expanding the distribution functions in moments and by deriving the evolution equations for moments from the Boltzmann equations. It turned out that both methods yield the Navier-Stokes equations as the first-order term, but there remains a serious problem that the resulting high-order equations beyond the first order may or may not be consistent with the thermodynamic laws. One of the reason for this problem is that the second law of thermodynamics is not fully incorporated into processes of these methods, even though it plays a critical role in yielding the phenomenologically correct solution.

On the other hand, Eu's generalized hydrodynamics are derived in a way that the resulting equations are completely consistent with the second law of thermodynamics to every order of approximations. For this reason, Eu's generalized hydrodynamics is taken as the basis for mathematical models in this study. For the detailed discussion of subtlety of the Boltzmann kinetic theory and Eu's generalized hydrodynamics, refer to Eu's original papers [8, 10].

3 Eu's Generalized Hydrodynamic Equations

3.1 Governing Equations

A thermodynamically consistent hydrodynamic computational model of the conserved and non-conserved variables has been developed by Myong [25], starting from Eu's generalized hydrodynamics. The dimensionless evolution equations of a monatomic gas can be written as

$$\mathbf{U}_t + \nabla \cdot \mathbf{F}_T = 0, \tag{1}$$

and

$$\hat{\mathbf{\Pi}}\, q(c\hat{R}) = \hat{\mathbf{\Pi}}_0 + [\hat{\mathbf{\Pi}} \cdot \nabla \hat{\mathbf{u}}]^{(2)}, \tag{2}$$

$$\hat{\mathbf{Q}}\, q(c\hat{R}) = \hat{\mathbf{Q}}_0 + \hat{\mathbf{\Pi}} \cdot \hat{\mathbf{Q}}_0, \tag{3}$$

where

$$\mathbf{U} = \begin{pmatrix} \rho \\ \rho\mathbf{u} \\ \rho E \end{pmatrix}, \mathbf{F} = \begin{pmatrix} \rho\mathbf{u} \\ \rho\mathbf{u}\mathbf{u} + \frac{1}{\gamma \mathrm{M}^2} p\mathbf{I} \\ (\rho E + \frac{1}{\gamma \mathrm{M}^2} p)\mathbf{u} \end{pmatrix}, \mathbf{F}_v = \frac{1}{\mathrm{Re}} \begin{pmatrix} 0 \\ \mathbf{\Pi} \\ \mathbf{\Pi} \cdot \mathbf{u} + \frac{1}{\mathrm{EcPr}} \mathbf{Q} \end{pmatrix},$$

and

$$\hat{\mathbf{\Pi}} \equiv \frac{\mathrm{N}_\delta}{p} \mathbf{\Pi},\ \hat{\mathbf{Q}} \equiv \frac{\mathrm{N}_\delta}{p} \frac{\mathbf{Q}}{\sqrt{T/(2\epsilon)}},\ \nabla \hat{\mathbf{u}} = -2\eta \frac{\mathrm{N}_\delta}{p} \nabla \mathbf{u},$$

$$\hat{R}^2 = \hat{\mathbf{\Pi}} : \hat{\mathbf{\Pi}} + \hat{\mathbf{Q}} \cdot \hat{\mathbf{Q}},\ q(c\hat{R}) = \frac{\sinh(c\hat{R})}{c\hat{R}},$$

$$\mathbf{\Pi}_0 = -2\eta [\nabla \mathbf{u}]^{(2)},\ \mathbf{Q}_0 = -\lambda \nabla \ln T,\ \epsilon = \frac{1}{\mathrm{PrEc} T_r / \triangle T}.$$

Here $\mathbf{U}$ is the vector of conserved variables, $\mathbf{F}_T$ represents the sum of the inviscid flux vector $\mathbf{F}$ and the viscous flux vector $\mathbf{F}_v$. ρ is the mass density, $\mathbf{u}$ is the fluid velocity, p is the pressure, T is the temperature, E is the total energy density, $\mathbf{\Pi}$ is the shear stress, and $\mathbf{Q}$ is the heat flux. The symbol $[\nabla \mathbf{u}]^{(2)}$ stands for the traceless symmetric part of a

tensor $\nabla\mathbf{u}$ and the term $[\mathbf{\Pi}\cdot\nabla\mathbf{u}]^{(2)}$ represents the coupling between the shear stress and velocity gradient tensor. It should be mentioned in the constitutive relation (3) that a term $\frac{1}{2\mathrm{Pr}}\hat{\mathbf{Q}}\cdot\nabla\hat{\mathbf{u}}$ appearing in the original constitutive relation of heat flux [25] is omitted for simplicity in the present study. M, Re, Ec, and Pr represent dimensionless numbers, Mach, Reynolds, Eckert, and Prandtl. The subscript r represents the reference state, for example, the state in inflow condition. A constant c, which is given as

$$c=\left[\frac{2\sqrt{\pi}}{5}A_2(\nu)\Gamma[4-2/(\nu-1)]\right]^{1/2}, \tag{4}$$

has a value between 1.0138 (Maxwellian) and 1.2232 (ν=3), where ν is the exponent of the inverse power laws of gas particles and $s=\frac{1}{2}+\frac{2}{\nu-1}$. $A_2(\nu)$ are pure numbers; tabulated values are available in textbooks of kinetic theory. η and λ are the Chapman-Enskog viscosity and thermal conductivity. They can be expressed as $\eta=T^s,\ \lambda=T^{s+1}$.

For a monatomic gas, $\gamma=\frac{5}{3}$ and $\mathrm{Pr}=\frac{2}{3}$. For perfect gas the following relations hold

$$p=\rho T,\ \rho E=\frac{p/(\gamma\mathrm{M}^2)}{(\gamma-1)}+\frac{1}{2}\rho\mathbf{u}\cdot\mathbf{u}. \tag{5}$$

A composite number, which is defined as $\mathrm{N}_\delta=\gamma\mathrm{M}^2/\mathrm{Re}=\mathrm{Kn}\,\mathrm{M}\sqrt{2\gamma/\pi}$, measures the magnitude of the viscous stress relative to the hydrostatic pressure, so that it indicates the level of departure from equilibrium. Through this number the new hydrodynamic equations (1)-(3) are able to take into account the effect of high Knudsen numbers. When N_δ becomes small, the constitutive relations (2) and (3) recovers

$$\mathbf{\Pi}=\mathbf{\Pi}_0\ \text{ and }\ \mathbf{Q}=\mathbf{Q}_0, \tag{6}$$

which is nothing but the Navier-Stokes-Fourier constitutive relations. It should be noted that the present constitutive relations are expressed in terms multiplied by

$$\frac{\mathrm{N}_\delta}{p}\mathbf{\Pi}\ \text{ or }\ \frac{\mathbf{\Pi}}{p}\ \text{ in dimensional form,}$$

which is the exact measure of non-equilibrium.

The unique feature of the new set of hydrodynamic equations is the existence of a highly nonlinear factor $q(c\hat{R})$ in the constitutive relations. It depends on a parameter $\hat{R}$, which measures the local level of non-equilibrium. The role of $q(c\hat{R})$ can be manifested once the entropy production is calculated. The entropy production for generalized hydrodynamics, which measures energy dissipation arising from molecular collisions, can be expressed as [10]

$$\sigma_{\text{ent}} \sim \hat{R}^2 q(c\hat{R}). \tag{7}$$

Since $\hat{R}^2$, which is the sum of the double product of stress tensor and the dot product of heat flux vector, and $q(c\hat{R})$ always remain positive, the entropy production is inherently positive, regardless of Knudsen numbers, order of approximations, and flow conditions.

Another feature is that the new equations are frame-independent, in other words, not dependent on the motion of the observer. This is related to the fact that the generalized hydrodynamic equations can be made co-rotational by using the Jaumann derivative [9]. Not all of the previous hydrodynamic equations do satisfy such property, whereas the Navier-Stokes equations always do.[2]

3.2 Boundary Conditions

The hydrodynamic equations (1)-(3) are subject to boundary conditions. The common practice in rarefied and microscale gasdynamics is to employ some type of slip boundary conditions, for example, the Maxwell-Smoluchowski condition. There exist growing evidences [2] that this slip boundary condition plays the most important role in determining

[2]There remains the general question of whether constitutive relations should be frame-independent or not. It was, however, generally accepted that correctly formulated constitutive relations were necessarily frame-independent [31].

the overall flowfield in microscale gas flows. It is based on the notion of accommodation coefficients which measure the slip effects at the solid boundary, depending upon the gradient of tangential velocity and temperature. Under isothermal assumption, it can be simplified as

$$u = u_w + \frac{2-\sigma}{\sigma}\frac{\mathrm{Kn}}{p}\Big(\frac{\partial u}{\partial n}\Big)_w \tag{8}$$

The subscript w represents the wall. The slip velocity depends on global Knudsen number, local pressure, accommodation coefficients σ, and normal gradient of tangential velocity. The case with $\sigma = 1$ represents perfect diffusive reflection. It should be, however, noticed that the slip velocity is unbounded since either the value of the Knudsen number divided by the local pressure or the normal gradient of tangential velocity can be very large.

It is also instructive to mention that owing to the introduction of adjustable coefficients σ this condition loses the predictability, so that handling the boundary condition for high-Knudsen-number gas flow becomes problem-dependent. There exist some calculations where the general solutions are highly dependent on the exact value of surface accommodation coefficients [21].

In the present study, a boundary condition is developed that recovers the predictability and facilitates hydrodynamic treatment of the entire density regime with a formalism. It is expected that the present method can avoid many problems residing in the Maxwell-Smoluchowski condition. The idea is to take the interfacial gas-surface molecule interactions into account and to let the flowfield determine the pressure at the gas-surface boundary. A fraction α of molecules reaching thermal equilibrium with the wall can be expressed as [4, 24]

$$\alpha = \frac{\beta p}{1+\beta p}, \tag{9}$$

where the parameter β depends on the wall temperature T_w and the interfacial interaction

parameters. By equalizing the gas-surface molecule interaction process with a chemical reaction β can be written as

$$\beta = \frac{Al_r}{k_B T_w} e^{\frac{D_e}{k_B T_w}} \cdot \frac{\ell}{l_r}, \tag{10}$$

where A is the mean area of a site, D_e is the potential parameter and they can be inferred from experimental data. l is the mean free path, and k_B is the Boltzmann constant. The subscript r represents the reference value such as the value at the free-stream or the local value adjacent to the surface. ℓ is a mean collision distance between the wall surface and the gas molecules at all angles [4]. When the characteristic length L is taken as ℓ, $\frac{\ell}{l_r}$ is equivalent to 1/Kn. When the free-stream mean free path is taken as ℓ, it becomes unity. With α calculated, the boundary values of temperature and velocity can be determined by

$$T = \alpha T_w + (1-\alpha) T_r, \tag{11}$$

$$u = \alpha u_w + (1-\alpha) u_r. \tag{12}$$

In multi-dimensional problem, u should be interpreted as the magnitude of the velocity vector. In contrast with the Maxwell-Smoluchowski condition the new condition does not involve the gradient of velocity and is always bounded by the reference value, which seems to be more physically sound. A simple expression for β can be obtained after some manipulation,

$$\beta = \sqrt{\frac{\pi}{32}} \frac{A}{c^2 d_{\mathrm{STP}}^2} \Big[\frac{T_r}{273}\Big]^{\frac{2}{\nu-1}} \frac{T_r}{T_w} e^{\frac{D_e}{k_B T_w}} \frac{\ell}{l_r} \frac{1}{p_r}. \tag{13}$$

Here l_r is defined as $(\pi/2)^{1/2} \eta_r (RT_r)^{-1/2}/\rho_r$. For an Ar-Al molecular interaction model,

$$D_e = 1.32\,\mathrm{kcal/mol},\ A = 5 \cdot 10^{-15}\,\mathrm{cm}^2,$$

$$d_{\mathrm{STP}} = 3.659 \cdot 10^{-8}\,\mathrm{cm}.$$

The parameter β reduces to

$$\beta = 1.1294 \left[\frac{T_r}{273}\right]^{\frac{1}{4}} \frac{1}{T_w/T_r}\, e^{\left[\frac{664.23}{T_r}\frac{1}{T_w/T_r}\right]} \frac{\ell}{l_r}\frac{1}{p_r}.$$

In Fig. 2, fraction of molecules reaching thermal equilibrium in the gas-surface interface as function of pressure is described in logarithmic scale. Finally, the wall pressure can be determined by putting the pressure gradient normal to the boundary zero.

In summary, the fraction α of molecules reaching equilibrium depends on Knudsen number, local pressure, free-stream and wall temperature, viscosity coefficient ν, and gas-surface parameters (D_e, A). With an interfacial gas-surface molecule interaction model the new hydrodynamic equations do not require any further condition beyond the boundary condition of the Navier-Stokes equations. As seen in the equations (2) and (3), the new relations involve only the first derivatives of velocity and temperature, so that they do not suffer the difficulty that often arises in other equations with higher-order derivative terms [18].

4 CFD Algorithms

The new hydrodynamic equations (1)-(3) are not different from the well-documented Navier-Stokes equations. Therefore, most of modern CFD schemes based on the Navier-Stokes equations can be applied. In present work, the upwind scheme with van Leer's flux vector splitting solver [29] is used since it is accurate and robust. Second-order accuracy can be obtained using the MUSCL-Hancock method [30]. With these algorithms on the conservation laws (1), an algorithm to solve the highly nonlinear constitutive relations (2) and (3) must be developed. It should provide the shear stresses and heat flux for given thermodynamic variables (pressure and temperature) and the gradient of velocity and temperature. Then the one-dimensional discretization form of the new hydrodynamic equations in finite

volume formulation can be expressed as

$$\mathbf{U}_i^{n+1} = \mathbf{U}_i^n - \frac{\triangle t}{\triangle x}\Big[\mathbf{F}^n_{T_{i+\frac{1}{2}}} - \mathbf{F}^n_{T_{i-\frac{1}{2}}}\Big], \tag{14}$$

where $\mathbf{U}$ is the cell-averaged conserved variables, $\triangle x$ is the size of i-cell, and $\mathbf{F}_T$ is the numerical flux function which gives the flux through cell interfaces. In finite volume formulation, the shear stress and heat flux are defined only on cell surfaces, so that the algebra in solving the constitutive equations is considerably reduced.

4.1 Solutions of Constitutive Relations

In general, the constitutive relations (2) and (3) consist of 9 equations of (Π_{xx}, Π_{xy}, Π_{xz}, Π_{yy}, Π_{yz}, Π_{zz}, Q_x, Q_y, Q_z) for given 12 parameters (∇u, ∇v, ∇w, ∇T). Owing to the highly nonlinear terms, it is not obvious whether they can be solved or not. It was shown, however, that they can be solved by a numerical method in one-dimensional problem [25]. The stress and heat flux components (Π_{xx}, Π_{xy}, Q_x) on a line in the two-dimensional physical plane induced by thermodynamic forces (u_x, v_x, T_x) can be approximated as the sum of two solvers: (1) one on (u_x, 0, T_x); and (2) another on (0, v_x, 0). In three-dimensional problem, (Π_{xx}, Π_{xy}, Π_{xz}, Q_x) on a surface can be approximated as the sum of two solvers: (1) one on (u_x, 0, 0, T_x); and (2) another on (0, v_x, w_x, 0). Here we present only two-dimensional case since it can be easily extended to three-dimensional problem by noting $(v_x, w_x) = (v\cos\theta, v\sin\theta)$ where $v = \sqrt{v_x^2 + w_x^2}$, $\theta = \tan^{-1}\frac{w_x}{v_x}$. In the previous work [25], it was shown that the equations for the first solver are given by

$$\hat{\Pi}_{xx} q(c\hat{R}) = (\hat{\Pi}_{xx} + 1)\hat{\Pi}_{xx_0}, \tag{15}$$

$$\hat{Q}_x q(c\hat{R}) = (\hat{\Pi}_{xx} + 1)\hat{Q}_{x_0}, \tag{16}$$

where $\hat{R}^2 = \frac{3}{2}\hat{\Pi}_{xx}^2 + \hat{Q}_x^2$. The factor 3/2 in $\hat{R}^2$ originates from

$$\hat{\Pi}_{yy} = \hat{\Pi}_{zz} = -\frac{1}{2}\hat{\Pi}_{xx}.$$

The equations for the second solver are given in the following form

$$\hat{\Pi}_{xx} q^2(c\hat{R}) \;\; = \;\; -\frac{2}{3}(\hat{\Pi}_{xx}+1)\hat{\Pi}_{xx_0}^2, \tag{17}$$

where $\hat{R}^2 = 3\hat{\Pi}_{xx}(\hat{\Pi}_{xx} - 1)$ from

$$\hat{\Pi}_{xx} = \hat{\Pi}_{zz} = -\frac{1}{2}\hat{\Pi}_{yy},$$

with a constraint

$$\hat{\Pi}_{xy} = \mathrm{sign}(\hat{\Pi}_{xy_0})\Big[-\frac{3}{2}(\hat{\Pi}_{xx}+1)\hat{\Pi}_{xx}\Big]^{1/2}. \tag{18}$$

These can be solved by the method of iteration, which turned out to provide converged solutions within a few iterations. The iteration procedures can be summarized as follows. For mathematical proof of convergence, refer to the previous work [25]. In the solver on $(u_x, 0, T_x)$, for positive $\hat{\Pi}_{xx}$ and $\hat{Q}_x$

$$\hat{R}_{n+1} = \frac{1}{c}\sinh^{-1}[c(\hat{\Pi}_{xx_n}+1)\hat{R}_0] \;\text{ and }\; \frac{\hat{Q}_{x_{n+1}}}{\hat{\Pi}_{xx_{n+1}}} = \frac{\hat{Q}_{x_n}}{\hat{\Pi}_{xx_n}} = \frac{\hat{Q}_{x_0}}{\hat{\Pi}_{xx_0}}, \tag{19}$$

and for negative $\hat{\Pi}_{xx}$ and $\hat{Q}_x$

$$\hat{\Pi}_{xx_{n+1}} = \frac{\hat{\Pi}_{xx_0}}{q(c\hat{R}_n) - \hat{\Pi}_{xx_0}} \;\text{ and }\; \hat{Q}_{x_{n+1}} = \frac{(\hat{\Pi}_{xx_n}+1)\hat{Q}_{x_0}}{q(c\hat{R}_n)}, \tag{20}$$

where $\hat{\Pi}_{xx_1}$ and $\hat{Q}_{x_1}$ are given by the equations

$$\hat{\Pi}_{xx_1} = \frac{\sinh^{-1}(c\hat{R}_0)}{c\hat{R}_0}\,\hat{\Pi}_{xx_0},\; \hat{Q}_{x_1} = \frac{\sinh^{-1}(c\hat{R}_0)}{c\hat{R}_0}\,\hat{Q}_{x_0}. \tag{21}$$

In the solver on $(0, v_x, 0)$, the $\hat{\Pi}_{xx}$ can be obtained for a given $\hat{\Pi}_{xy_0}$ through

$$\hat{\Pi}_{xx_{n+1}} = -\frac{\hat{\Pi}_{xy_0}^2}{3q^2(c\hat{R}_n)/2 + \hat{\Pi}_{xy_0}^2}. \tag{22}$$

The $\hat{\Pi}_{xy}$ can be calculated using the constraint relation (18).

The general properties are shown in Fig. 3. The Fig. 3 (a) shows the asymmetry of normal stress for rapid expansion and compression of gas. In this figure heat flux is assumed zero for simplicity. It has been reported that the augmented conventional Burnett equations produce a severe instability near the point where the flow separated at the shoulder of the hypersonic vehicles [22]. It was suggested that the instability is caused by the problems that a rapidly expanding gas exhibits negative entropy production in the Burnett-type formulations. By contrast, the new relations will not suffer such instability since they always yield positive entropy production. The Fig. 3 (b) demonstrated that $(\hat{\Pi}_{xx} + 1)$ or $(\Pi_{xx} + p/\mathrm{N}_\delta)$, and $\hat{\Pi}_{xy}$ of new relations approach zero as the tangential velocity gradient becomes very large. Such asymptotic behavior indicates that the new relations have a correct free-molecular limit, implying that the velocity-slip phenomenon can be explained in purely hydrodynamic terms. The details of properties of the new constitutive relations are given in the previous work [25].

4.2 Numerical Flux in Finite Volume Formulation

It was not yet described how the numerical flux through the interface in the equation (14) can be calculated in general non-Cartesian domains. It can be determined by exploiting the rotational invariance of the conservation laws (1).

Let consider the k-th intercell boundary $\triangle L_k$ of finite area $A_{i,j}$ in two-dimensional (x, y) space. Let define $\mathbf{n}_k, \mathbf{s}_k$ the outward unit vector normal to the k-th boundary, and the unit vector tangent to the k-th boundary with convention that the interior of the volume always lies on the left hand side of the boundary. If θ_k is defined as the angle formed by the

x-direction and the normal vector $\mathbf{n}_k$, it can be shown that the equation (14) becomes

$$\mathbf{U}_{i,j}^{n+1} = \mathbf{U}_{i,j}^{n} - \frac{\triangle t}{A_{i,j}} \sum_{k=1}^{N} \mathbf{R}_k^{-1} \mathbf{F}_{T_k}^{n} \triangle L_k, \tag{23}$$

where

$$\mathbf{U}_{i,j} = \begin{pmatrix} \rho \\ \rho u \\ \rho v \\ \rho E \end{pmatrix}_{i,j}, \mathbf{F}_{T_k} = \begin{pmatrix} \rho u_n \\ \rho u_n^2 + \frac{1}{\gamma \mathrm{M}^2} p \\ \rho u_n u_s \\ (\rho E + \frac{1}{\gamma \mathrm{M}^2} p) u_n \end{pmatrix}_k + \frac{1}{\mathrm{Re}} \begin{pmatrix} 0 \\ \Pi_{nn} \\ \Pi_{ns} \\ \Pi_{nn} u_n + \Pi_{ns} u_s + \frac{1}{\mathrm{EcPr}} Q_n \end{pmatrix}_k,$$

and $\mathbf{R}_k \equiv \mathbf{R}(\theta_k)$ is the rotation matrix, namely,

$$\mathbf{R}(\theta) = \begin{pmatrix} 1 & 0 & 0 & 0 \\ 0 & \cos\theta & \sin\theta & 0 \\ 0 & -\sin\theta & \cos\theta & 0 \\ 0 & 0 & 0 & 1 \end{pmatrix}.$$

N is the number of interface in a cell. In this process, a transformation law between the components of the tensor in (x, y) coordinates ($\mathbf{\Pi}$) and the components of the tensor in (n, s) coordinates ($\mathbf{\Pi}^*$) is used [12].

$$\mathbf{\Pi} = \mathbf{R}^{-1} \mathbf{\Pi}^* \mathbf{R} \tag{24}$$

The extension to three-dimension problem is also straightforward. Let consider the l-th intercell surface boundary $\triangle S_l$ of finite volume $V_{i,j,k}$ in three-dimensional (x, y, z) space. Let define $(\mathbf{n}, \mathbf{s}, \mathbf{t})_l$ the outward unit vector normal to the l-th boundary, and the unit vectors tangent to the l-th boundary with convention that the interior of the volume always lies on the left hand side of the boundary. If $\theta^{(z)}$ and $\theta^{(y)}$ are defined as rotational angles about the z and y axis, it can be shown that the equation (14) becomes

$$\mathbf{U}_{i,j,k}^{n+1} = \mathbf{U}_{i,j,k}^{n} - \frac{\triangle t}{V_{i,j,k}} \sum_{l=1}^{N} \mathbf{R}_l^{-1} \mathbf{F}_{Tl}^{n} \triangle S_l, \tag{25}$$

where

$$\mathbf{U}_{i,j,k} = \begin{pmatrix} \rho \\ \rho u \\ \rho v \\ \rho w \\ \rho E \end{pmatrix}_{i,j,k}, \mathbf{F}_{T_l} = \begin{pmatrix} \rho u_n \\ \rho u_n^2 + \frac{1}{\gamma \mathrm{M}^2} p \\ \rho u_n u_s \\ \rho u_n u_t \\ (\rho E + \frac{1}{\gamma \mathrm{M}^2} p) u_n \end{pmatrix}_l + \frac{1}{\mathrm{Re}} \begin{pmatrix} 0 \\ \Pi_{nn} \\ \Pi_{ns} \\ \Pi_{nt} \\ \Pi_{nn} u_n + \Pi_{ns} u_s + \Pi_{nt} u_t + \frac{1}{\mathrm{EcPr}} Q_n \end{pmatrix}_l,$$

and $\mathbf{R}_l$ is the rotation matrix, given as,

$$\mathbf{R} = \mathbf{R}^{(y)}\mathbf{R}^{(z)}$$

where

$$\mathbf{R}^{(y)} = \begin{pmatrix} 1 & 0 & 0 & 0 & 0 \\ 0 & \cos\theta^{(y)} & 0 & \sin\theta^{(y)} & 0 \\ 0 & 0 & 1 & 0 & 0 \\ 0 & -\sin\theta^{(y)} & 0 & \cos\theta^{(y)} & 0 \\ 0 & 0 & 0 & 0 & 1 \end{pmatrix}, \mathbf{R}^{(z)} = \begin{pmatrix} 1 & 0 & 0 & 0 & 0 \\ 0 & \cos\theta^{(z)} & \sin\theta^{(z)} & 0 & 0 \\ 0 & -\sin\theta^{(z)} & \cos\theta^{(z)} & 0 & 0 \\ 0 & 0 & 0 & 1 & 0 \\ 0 & 0 & 0 & 0 & 1 \end{pmatrix}.$$

Similar to the two-dimensional case, the components of the tensor in (x, y, z) coordinates ($\mathbf{\Pi}$) are related to the components of the tensor in (n, s, t) coordinates ($\mathbf{\Pi}^*$) through the transformation law (24).

4.3 Time Step and Numerical Boundary Conditions

For the generalized hydrodynamic equations, it turns out that the following stability condition for upwind schemes works well:

$$\triangle t = \mathrm{CFL} \cdot \min(\triangle t_1, \triangle t_2) \tag{26}$$

where

$$\triangle t_1 = \mathrm{M}\Big[\frac{\triangle x}{|a|} + \frac{2\eta\mathrm{M}}{\rho a^2}\Big],\ \triangle t_2 = \mathrm{M}\Big[\frac{|a|}{\triangle x} + \frac{\eta\mathrm{M}}{\rho \triangle x^2}\Big]^{-1}.$$

Notice that there exist Mach numbers in these relations. The reason is that the characteristic speed becomes a/M in dimensionless form, instead of a.

For given T_w, T_r, u_w, u_r, and p_r, the equations (11) and (12), and the mechanical balance condition $\frac{\partial p}{\partial n} = 0$ yield the boundary values of temperature, tangential velocity, and pressure. From these values, the boundary value of the density can be determined by the perfect gas relation. The velocity normal to the surface can be assumed to be zero. For artificial boundaries, inflow and outflow conditions based on the number of Euler characteristics can be employed.

5 Numerical Experiment: Shock Structure and Flat Plate Flow Computations

To demonstrate the capability of the new hydrodynamic equations, two challenging problems are considered. The gas is assumed as Argon ($s = 0.75$ in the coefficient of viscosity or $\nu = 9$, $c = 1.0179$ [25]) in all test cases. In general, the initial data necessary to define a well-posed problem consist of dimensionless parameters (M, Kn or Re), thermodynamic values (T_w, T_∞), gas properties (s or ν, d_{STP}, Pr, γ), and gas-surface molecular interaction parameters (D_e, A).

5.1 Shock Structure Problem

One is the hypersonic shock structure problem [1, 11, 14]. Even though this problem does not involve any solid boundary which may make the problem complicated, it has been known that the numerical calculation of the hypersonic shock structure presents serious theoretical and computational challenges. Here the shock structure is computed for a very high Mach number (M = 30) with a grid of 400 points. In Fig. 4, the shock profiles are illustrated. The second-order accuracy was maintained in this computation. 0.5 is used for the CFL number. A steady-state solution was considered to be obtained when the rms norm for the density dropped below 10^{-8}. The general configuration of the shock, which can be represented by the inverse shock thickness, seems to be in strong agreement with the results based on the DSMC calculation. For more details of Eu's generalized hydrodynamic results on this problem, see Al-Ghoul and Eu's work based on the system of ordinary differential equations [1] and Myong's work based on the system of partial differential equations [25].

5.2 Two-Dimensional Flat Plate Flow

Another is the hypersonic rarefied flat plate flow [21, 28, 32] in which the so-called slip phenomenon is important mechanism in determining the overall flow properties. This problem is one of fundamental interest since it generates a wide range of basic flow phenomena, for example, shock waves and slip flow.

In Figs. 5 and 6, the hypersonic rarefied flat plate flows ($\mathrm{M} = 12.9, \mathrm{Kn} = 0.0067, T_w = 5.4T_\infty, T_\infty = 200\mathrm{K}$) are described. The computational domain is defined by a rectangle of the size 1.25×0.4 with an equally-spaced grid of 120×48 points. It was checked by increasing the grid points whether the numerical results converge. Instead of the so-called Maxwell-Smoluchowski condition, a gas-surface (Ar-Al) molecular interaction model is used that depends on the pressure and temperature and provides the boundary values of temperature and velocity. ℓ is taken as the free-stream mean free path in this problem. The mirror boundary before the wall was introduced to prevent the disturbance affecting the inflow boundary. The boundary condition at the outflow was specified by extrapolation. The slip condition on the wall was applied by defining the dual ghost cells, one for the inviscid part where the boundary values of velocity and temperature are specified, and another for the viscous part where the values at the wall are used. Due to the large difference between the wall and free-stream temperature, a relatively small CFL number (0.1) is used. Since our main interest is to develop a multi-dimensional numerical method for Eu's generalized hydrodynamics, the first-order accuracy was maintained throughout the computational domain including the boundaries for simplicity. More study will be needed on the second-order accuracy upgrade and effects of boundary conditions. The exactly same conditions are applied to both Navier-Stokes and generalized hydrodynamics codes.

Numerical experiments indicated that the computing time of the two-dimensional gen-

eralized hydrodynamics code is comparable to that of the Navier-Stokes code. Overload, which is caused by the addition of a few iterations of constitutive relations (less than ten in most cases), occupies a small fraction of computing time in the code.

It seems that the general flow properties are similar to the result [32] based on the DSMC calculation. The contours of density show the separation of the oblique shock wave and the boundary layer. The density increases across the shock, but it then decreases. The maximum line of density can be observed in both Navier-Stokes and generalized hydrodynamic results. The Mach contours show that the velocity slip is large near the edge and become small in the latter half of the plate. The slip is slightly larger in the case of generalized hydrodynamics. It should be also noted that the generalized hydrodynamic results are less smooth near the leading edge than the Navier-Stokes results. It may be caused by the fact that the high gradient surface in the case of generalized hydrodynamics is not well aligned with the grid lines. In addition, it should be mentioned that the Maxwell-Smoluchowski boundary condition and the hard sphere particle model were used in the result of Yasuhara *et al.* [23]. Therefore, the direct comparison may not give much information of the generalized hydrodynamics in flat plate flow. Nonetheless, some interesting results can be found from the comparison between Navier-Stokes and generalized hydrodynamics calculations. As seen in Fig. 7, the Navier-Stokes calculation yields larger skin-friction and heat flux near the leading edge of the flat plate. On the contrary, the generalized hydrodynamics calculation produces more realistic results, removing the singularity near the leading edge that is ill-defined in continuum gas dynamics. The ultimate reason for this can be traced to the fact that through the relations (2) and (3) the stresses are nonlinearly related to the gradient of velocity in non-equilibrium flow regions.

6 Summary and Discussion

As a step towards developing reliable high-order fluid dynamic computational models for rarefied and microscale gas flows, Eu's generalized hydrodynamic equations have been studied. The numerical results using the multi-dimensional computational method for the thermodynamically consistent Eu's generalized hydrodynamic equations are presented. The main emphasis is placed on the development of a multi-dimensional finite volume method for the highly nonlinear Eu's generalized hydrodynamic equations. New insight into nonlinear transport process has been gained through the study of the hypersonic rarefied shock structure and flat plate flow. In this process a new boundary condition that does not need adjustable accommodation parameters is developed by taking the gas-surface molecule interaction into account. The study showed that the new equations yield more realistic solutions in highly non-equilibrium gas flows compared with the Navier-Stokes equations.

The main motivation of this study was to deal with three fundamental questions that need to be answered when addressing how highly non-equilibrium gas flows should be computed: (1) what is the appropriate set of high-order fluid dynamic equations in place of the Navier-Stokes equations?; (2) what are the boundary conditions suitable for this system?; and (3) what numerical method should be used to efficiently solve the system of nonlinear transport equations and the accompanying boundary conditions? In this study, the main emphasis is placed on the physical reasoning, which concerns of what physical elements or mathematical equations are essential, not on the choice of particular equations or methods. There can be many alternatives to the method taken in the present study.

However, the reasoning behind the present method will remain important. For the question (1), our reasoning is that the irreversible thermodynamics plays a fundamental role in deriving hydrodynamic equations from the Boltzmann equation, since the Boltzmann's

H-theorem is a much broader theorem pertaining to the molecular evolution of any system– not necessarily the system of gas molecules. In other words, the key bridge to make the kinetic theory so powerful in explaining nonlinear transport of gases is its connection to the thermodynamics. Therefore, we argue that any higher-order fluid dynamic equations should be formulated such that they satisfy the second law of thermodynamics for all conditions. For the question (2), the emphasis is placed on the conceptual consistency of boundary conditions. For example, it was checked whether the slip velocity remains bounded in the limit of free-molecular flow. In addition, by realizing that the rapidly changing profiles near the surface can be explained in purely hydrodynamic terms by thermodynamically consistent generalized hydrodynamic equations, we introduced a boundary condition that does not depend on parameters in bulk regime like the velocity gradient. For the question (3), our choice was to try to solve Eu's generalized hydrodynamic equations in form of parabolic type. The reason for this is that there exists no preferential direction of high-order moments (shear stress and heat flux).

Extension to more complicated gases will present non-trivial challenges. For example, the rotational non-equilibrium effect in diatomic gases will make the constitutive equations more complicated. It is also expected that the work involving gas mixture will become considerably difficult. Nonetheless, the basis of the present method will remain as the starting point towards developing thermodynamically consistent computational methods for high-Knudsen-number gas flows. After all, the main role of high-order terms is to increase the entropy, so that the physical law of explaining it should be taken into account in all steps. The present study shows that it is indeed possible to develop such methods.

Acknowledgments

This work was performed while the author held a visiting scholarship in Institute for Mathematics and its Applications of University of Minnesota (1999-2000 Program: Reactive Flow and Transport Phenomena). The work was also supported in part by Korea Science and Engineering Foundation under Research Grant 1999-2-305-001-3. The author wishes to express his deep appreciation to Professor B. C. Eu for his encouragement and advice.

References

[1] Al-Ghoul, M, and Eu, B. C., *Generalized hydrodynamics and shock waves*, Physical Review E, 56-3 (1997), pp. 2981–2992.

[2] Arkilic, E. B., Schmidt, M. A., and Breuer, K. S., *Gaseous slip flow in long microchannels*, IEEE J. MEMS, 6-2 (1997), pp. 167–178.

[3] Balakrishnan, R., Agarwal, R. K., and Yun, K. Y., *High-order distribution functions, BGK-Burnett equations and Boltzmann's H-theorem*, Paper 97-2551, AIAA, 1997.

[4] Bhattacharya, D. K., and Eu, B. C., *Nonlinear transport processes and fluid dynamics: Effects of thermoviscous coupling and nonlinear transport coefficients on plane Couette flow of Lennard-Jones fluids*, Physical Review A, 35-2 (1987), pp. 821–836.

[5] Bird, G. A., *Molecular gas dynamics and the direct simulation of gas flows*, Clarendon Press, Oxford, England, 1994.

[6] Brown, S., *Approximate Riemann solvers for moment models of dilute gases*, Ph.D. Thesis, The University of Michigan, 1996.

[7] Comeaux, K. A., Chapman, D. R., and MacCormack, R. W., *An analysis of the Burnett equations based on the second law of thermodynamics*, Paper 95-0415, AIAA, 1995.

[8] Eu, B. C., *A modified moment method and irreversible thermodynamics*, J. Chem. Phys., 73-6 (1980), pp. 2958–2969.

[9] Eu, B. C., *On the corotating frame and evolution equations in kinetic theory*, J. Chem. Phys., 82-8 (1985), pp. 3773–3778.

[10] Eu, B. C., *Kinetic theory and irreversible thermodynamics*, John Wiley & Sons, Inc., New York, 1992.

[11] Fiscko, K. A., and Chapman, D. R., *Comparison of Burnett, super-Burnett and Monte Carlo solutions for hypersonic shock structure*, Progress in Astronautics and Aeronautics, 118 (1989), pp. 374–395.

[12] Goodbody, A. M., *Cartesian tensors: With applications to mechanics, fluid mechanics and elasticity*, Ellis Horwood Ltd., Chichester, England, 1982.

[13] Grad, H., *On the kinetic theory of rarefied gases*, Comm. Pure Appl. Math., 2 (1949), pp. 331–407.

[14] Grad, H., *The profile of a steady plane shock wave*, Comm. Pure Appl. Math., 5 (1952), pp. 257–300.

[15] Ho, C. M., and Tai, Y. C., *Micro-electro-mechanical-systems (MEMS) and fluid flows*, Annu. Rev. Fluid Mech., 30 (1998), pp. 579–612.

[16] Ivanov, M. S., and Gimelshein, S. F., *Computational hypersonic rarefied flows*, Annu. Rev. Fluid Mech., 30 (1998), pp. 469–505.

[17] Koplik, J., and Banavar, J. R., *Continuum deductions from molecular hydrodynamics*, Annu. Rev. Fluid Mech., 27 (1995), pp. 257–292.

[18] Lee, C. J., *Unique determination of solutions to the Burnett equations*, AIAA J., 32-5 (1994), pp. 985–990.

[19] Levermore, C. D., *Moment closure hierarchies for kinetic theories*, J. of Statistical Phys., 83 (1996), pp. 1021–1065.

[20] Levermore, C. D., and Morokoff, W. J., *The Gaussian moment closure for gas dynamics*, SIAM J. Appl. Math., 59-1 (1998), pp. 72–96.

[21] Lord, R. G., *Direct simulation of rarefied hypersonic flow over a flat plate with incomplete surface accommodation*, Progress in Astronautics and Aeronautics, 160 (1992), pp. 221–228.

[22] Lumpkin, F. E., III, Boyd, I. D., and Venkatapathy, E., *Comparison of continuum and particle simulations of expanding rarefied flows*, Paper 93-0728, AIAA, 1993.

[23] Muller, I., *Extended thermodynamics*, Springer-Verlag, New York, 1993.

[24] Myong, R. S., *A new hydrodynamic approach to computational hypersonic rarefied gasdynamics*, Paper 99-3578, AIAA, 1999.

[25] Myong, R. S., *Thermodynamically-consistent hydrodynamic computational models for high-Knudsen-number gas flows*, Physics of Fluids, 11-9 (1999), pp. 2788–2802.

[26] Oran, E. S., Oh, C. K. and Cybyk, B. Z., *Direct simulation Monte Carlo: Recent advances and applications*, Annu. Rev. Fluid Mech., 30 (1998), pp. 403–441.

[27] Roveda, R., Goldstein, D. B., and Varghese, P. L., *Hybrid Euler/particle approach for continuum/rarefied flows*, J. Spacecraft and Rockets, 35-3 (1998), pp. 258–265.

[28] Tannehill, J. C., and Mohling, R. A., *Numerical computation of the hypersonic rarefied flow near the sharp leading edge of a flat plate*, Paper 73-200, AIAA, 1973.

[29] van Leer, B., *Flux-vector splitting for the Euler equations*, Technical Report ICASE 82-30, NASA Langley Research Center, U.S.A., 1982.

[30] van Leer, B., *On the relation between the upwind-differencing schemes of Godunov, Enguist-Osher and Roe*, SIAM J. Sci. Stat. Comput., 5-1 (1985), pp. 1–20.

[31] Woods, L. C., *Frame-indifferent kinetic theory*, J. Fluid Mech., 136 (1983), pp. 423–433.

[32] Yasuhara, M., Nakamura, Y., and Tanaka, J., *Monte Carlo simulation of flow into channel with sharp leading edge*, Progress in Astronautics and Aeronautics, 118 (1989), pp. 582–596.

Figure captions

Fig. 1. Mathematical models and solution methods for the description of the motion of gases.

Fig. 2. Fraction of molecules reaching thermal equilibrium in the interface as function of pressure in logarithmic scale ($\ell = L = 1\mu m, T_w = 300K$).

Fig. 3. (a) Generalized hydrodynamic constitutive relations relative to the Navier-Stokes relations (Argon, u_x only, no heat flux) (top). The horizontal and vertical axes represent the Navier-Stokes relations $\hat{\Pi}_{xx_0}$, and the new relations $\hat{\Pi}_{xx}$, respectively. The gas is expanding in the range $\hat{\Pi}_{xx_0} < 0$, whereas the gas is compressed in the range of $\hat{\Pi}_{xx_0} > 0$. (b) Generalized hydrodynamic constitutive relations relative to the Navier-Stokes relations (Argon, v_x only) (bottom). The horizontal axis represents the velocity gradient $\hat{v}_x/2$ or $\hat{\Pi}_{xy_0}$. The vertical axis represents the normal ($\hat{\Pi}_{xx}$) and shear ($\hat{\Pi}_{xy}$) stresses by new relations.

Fig. 4. Mach 30 shock profiles of normalized variables for Argon gas. Solid line with circle: generalized hydrodynamics (GH), solid line: Navier-Stokes (NS). The horizontal axis represents the spatial coordinate reduced by the mean free path (l) at the upstream condition. The inverse of the shock density thickness (GH - 0.1743, NS - 0.2152).

Fig. 5. Contours of constant density. (a) Generalized hydrodynamics (top). (b) Navier-Stokes (bottom). The solid wall begins at $x/L = 0$, where L is the length of the plate ($L = 150l_\infty$).

Fig. 6. Contours of Mach number. (a) Generalized hydrodynamics (top). (b) Navier-Stokes (bottom). The solid wall begins at $x/L = 0$, where L is the length of the plate ($L = 150l_\infty$).

Fig. 7. Properties near the plate. (a) Shear stress (top). (b) Heat flux (bottom). The solid wall begins at $x/L = 0$.

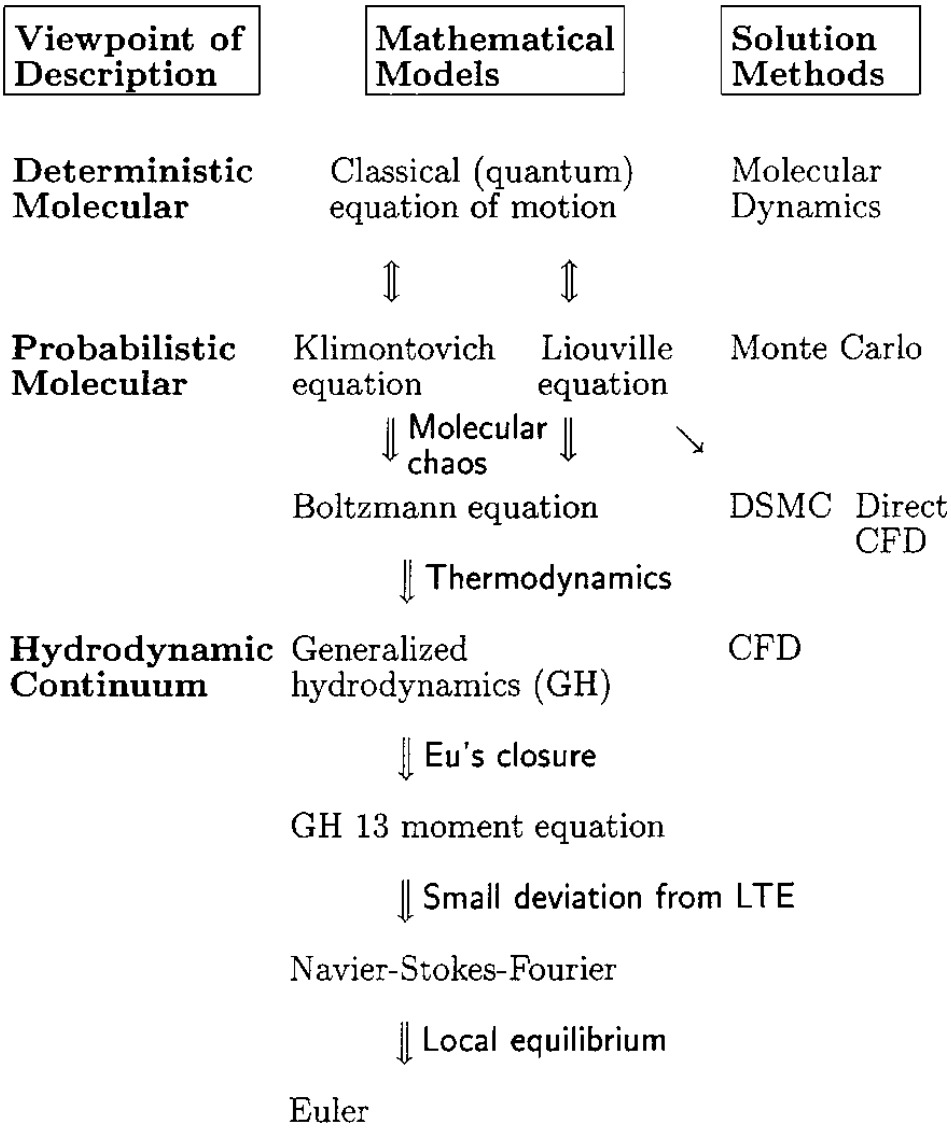
Viewpoint of Description
Mathematical Models
Solution Methods
Deterministic Molecular
Classical (quantum) equation of motion
Molecular Dynamics
Probabilistic Molecular
Klimontovich equation
Liouville equation
Monte Carlo
Molecular chaos
Boltzmann equation
DSMC
Direct CFD
Thermodynamics
Hydrodynamic Continuum
Generalized hydrodynamics (GH)
CFD
Eu's closure
GH 13 moment equation
Small deviation from LTE
Navier-Stokes-Fourier
Local equilibrium
Euler

Fig. 1

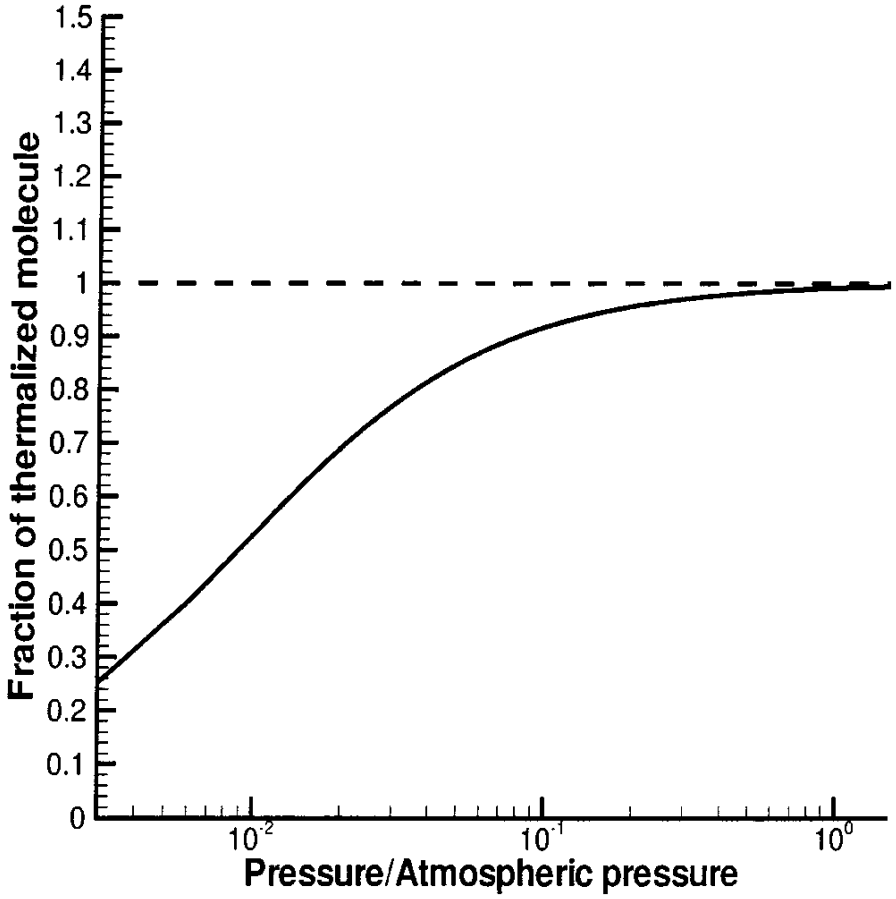
Fraction of thermalized molecule
1.5
1.4
1.3
1.2
1.1
1
0.9
0.8
0.7
0.6
0.5
0.4
0.3
0.2
0.1
0
10^{-2}
10^{-1}
10^{0}
Pressure/Atmospheric pressure

Fig. 2

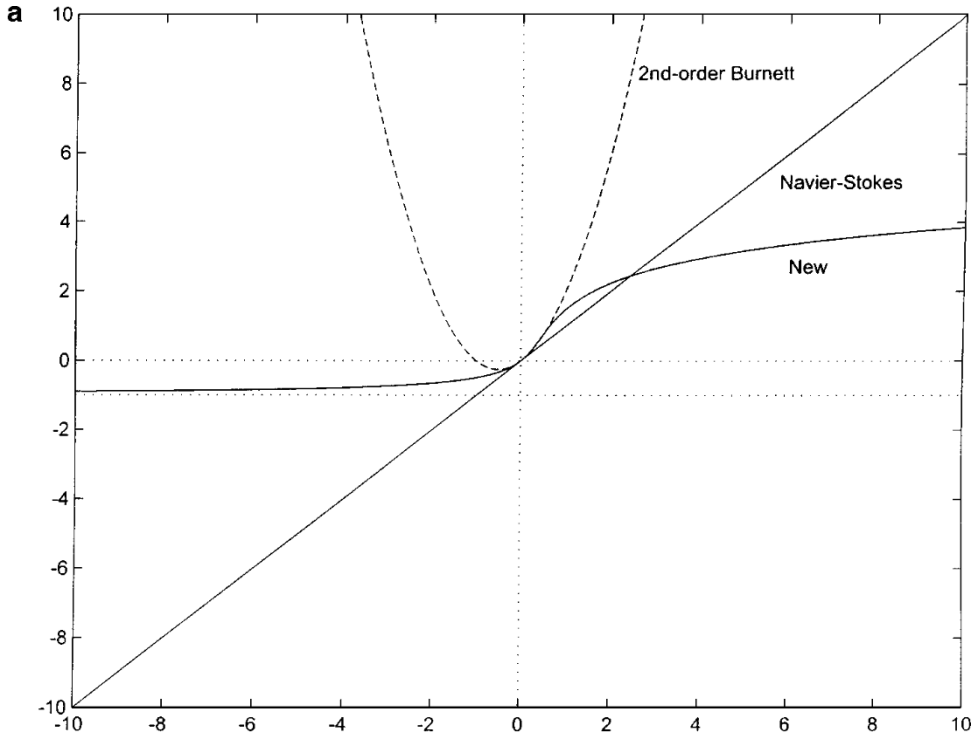
a
2nd-order Burnett
Navier-Stokes
New
10
8
6
4
2
0
-2
-4
-6
-8
-10
-10
-8
-6
-4
-2
0
2
4
6
8
10

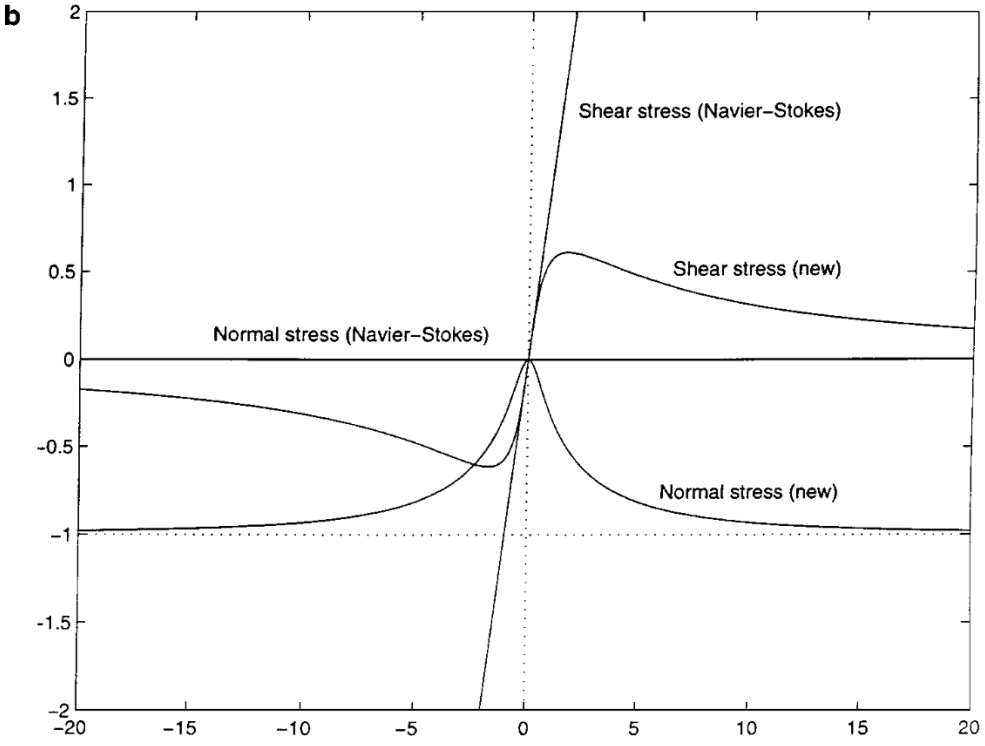
b
Shear stress (Navier–Stokes)
Shear stress (new)
Normal stress (Navier–Stokes)
Normal stress (new)

Fig. 3

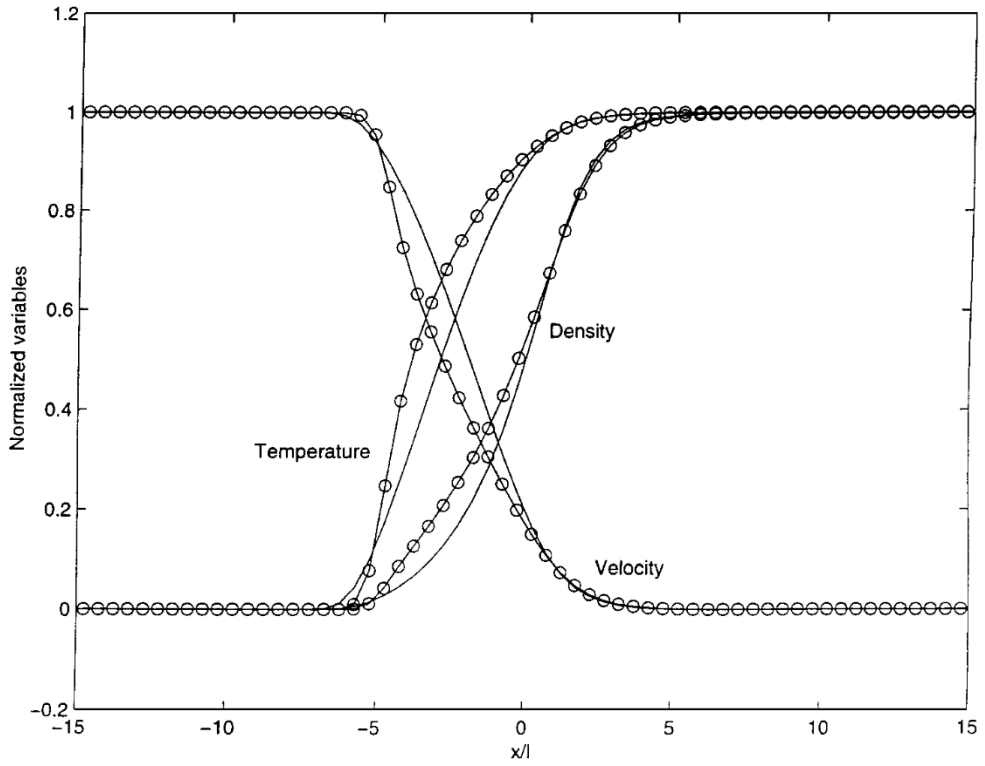
Normalized variables
Density
Temperature
Velocity
x/l

Fig. 4

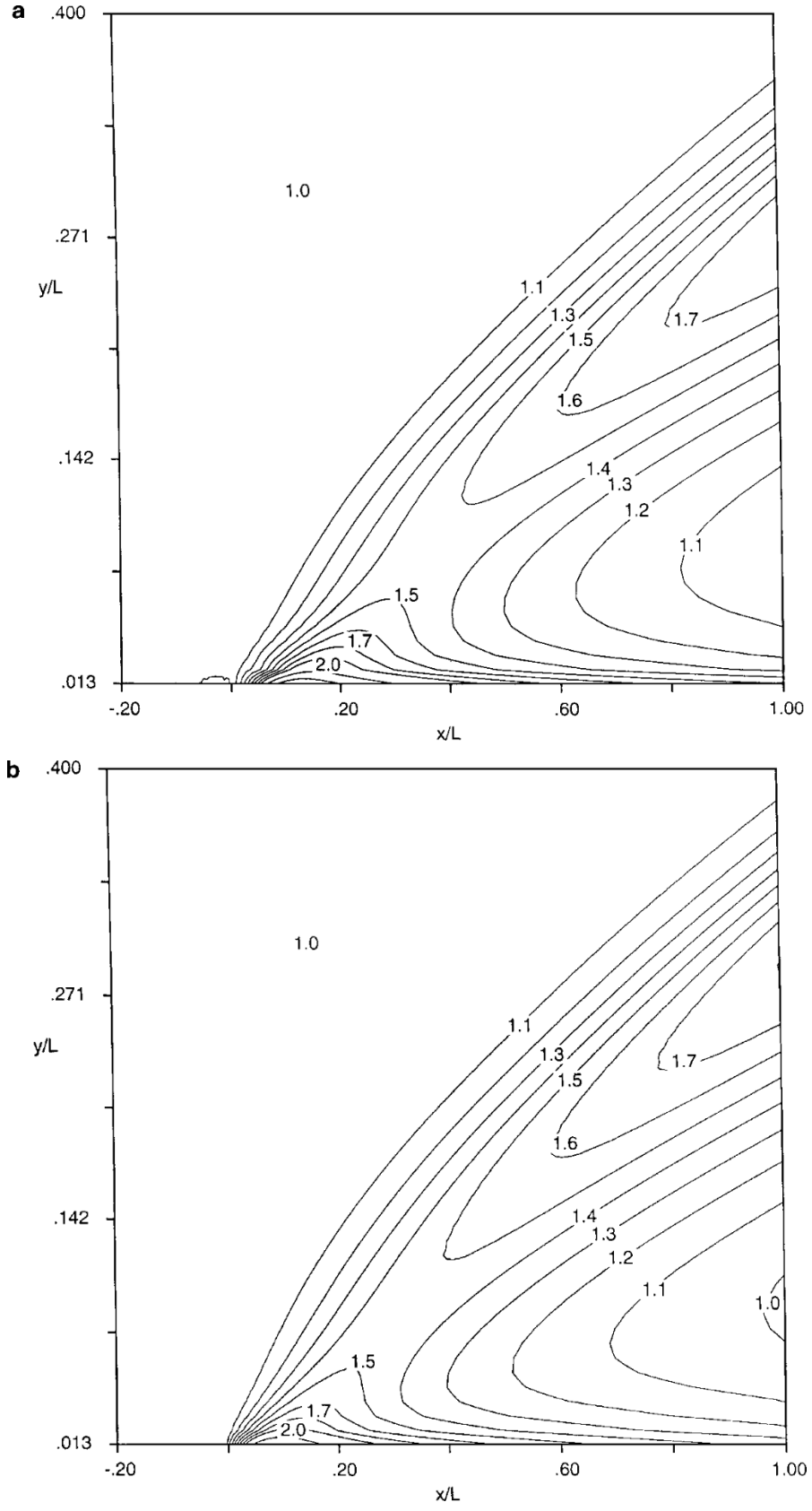
a
.400
.271
.142
.013
y/L
1.0
1.1
1.3
1.5
1.7
1.6
1.4
1.3
1.2
1.1
1.5
1.7
2.0
-.20
.20
.60
1.00
x/L
b
.400
.271
.142
.013
y/L
1.0
1.1
1.3
1.5
1.7
1.6
1.4
1.3
1.2
1.1
1.0
1.5
1.7
2.0
-.20
.20
.60
1.00
x/L

Fig. 5

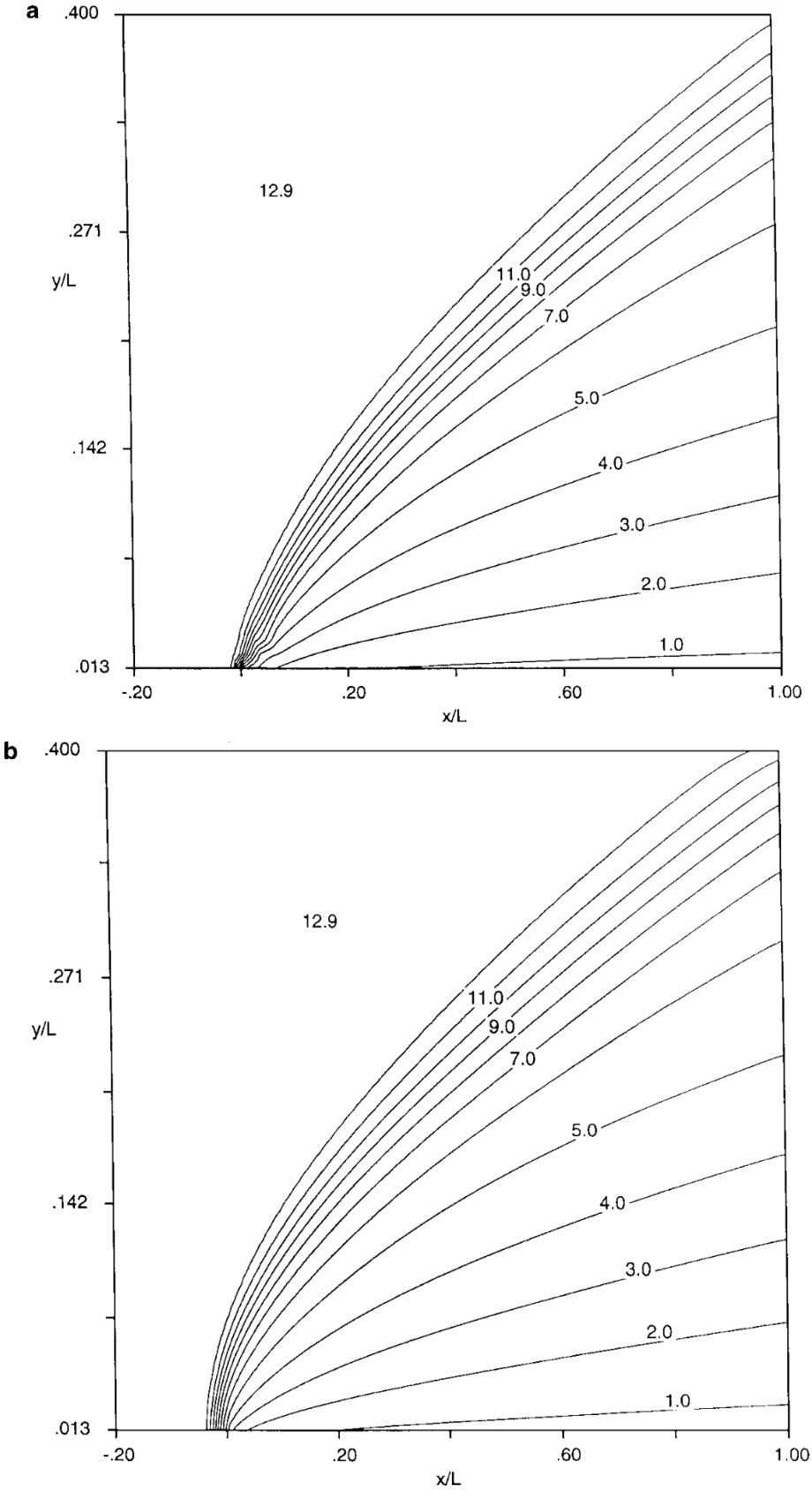
a
.400
.271
.142
.013
y/L
12.9
11.0
9.0
7.0
5.0
4.0
3.0
2.0
1.0
-.20
.20
.60
1.00
x/L
b
.400
.271
.142
.013
y/L
12.9
11.0
9.0
7.0
5.0
4.0
3.0
2.0
1.0
-.20
.20
.60
1.00
x/L

Fig. 6

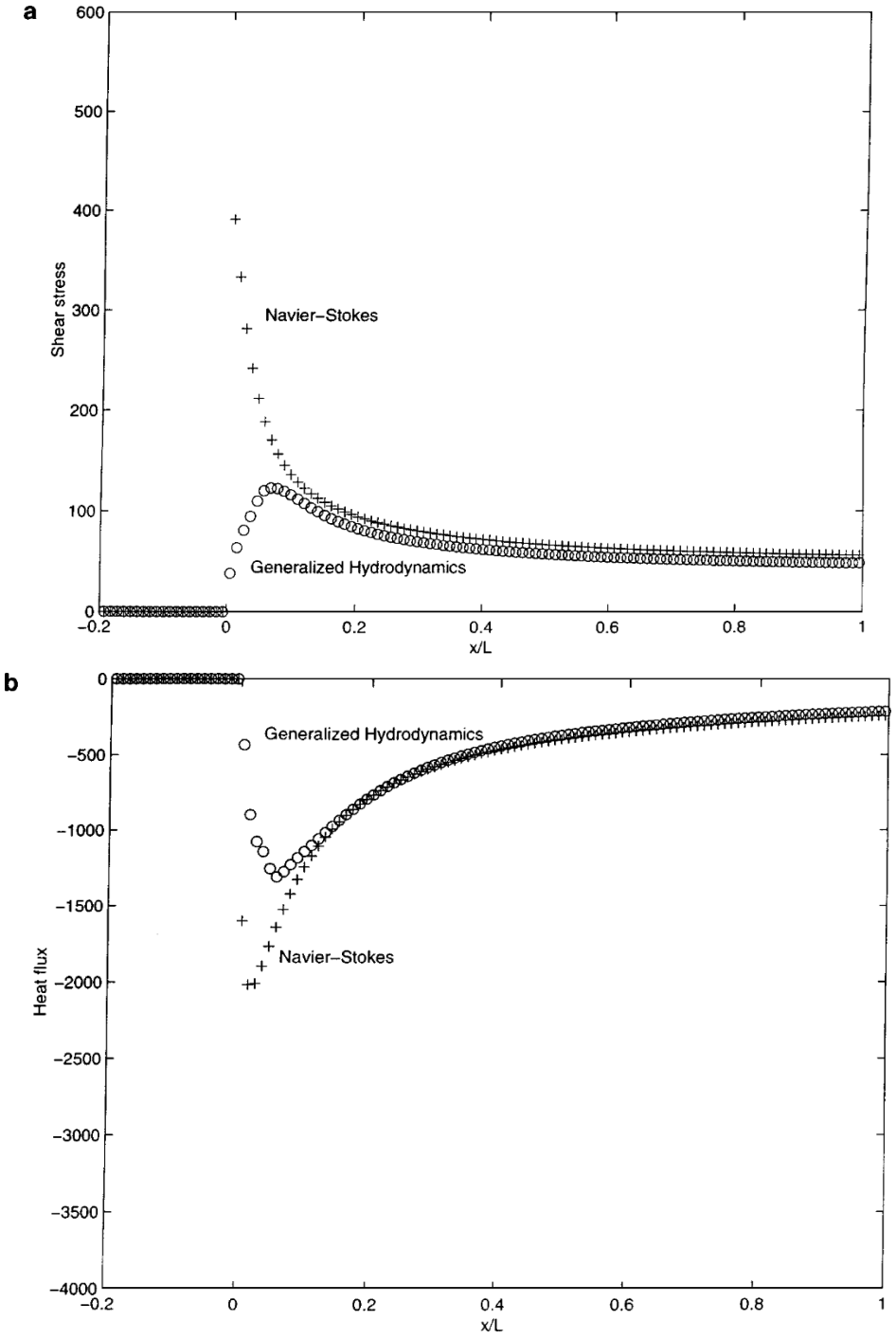
a
Shear stress
Navier–Stokes
Generalized Hydrodynamics
x/L
b
Heat flux
Generalized Hydrodynamics
Navier–Stokes
x/L

Fig. 7

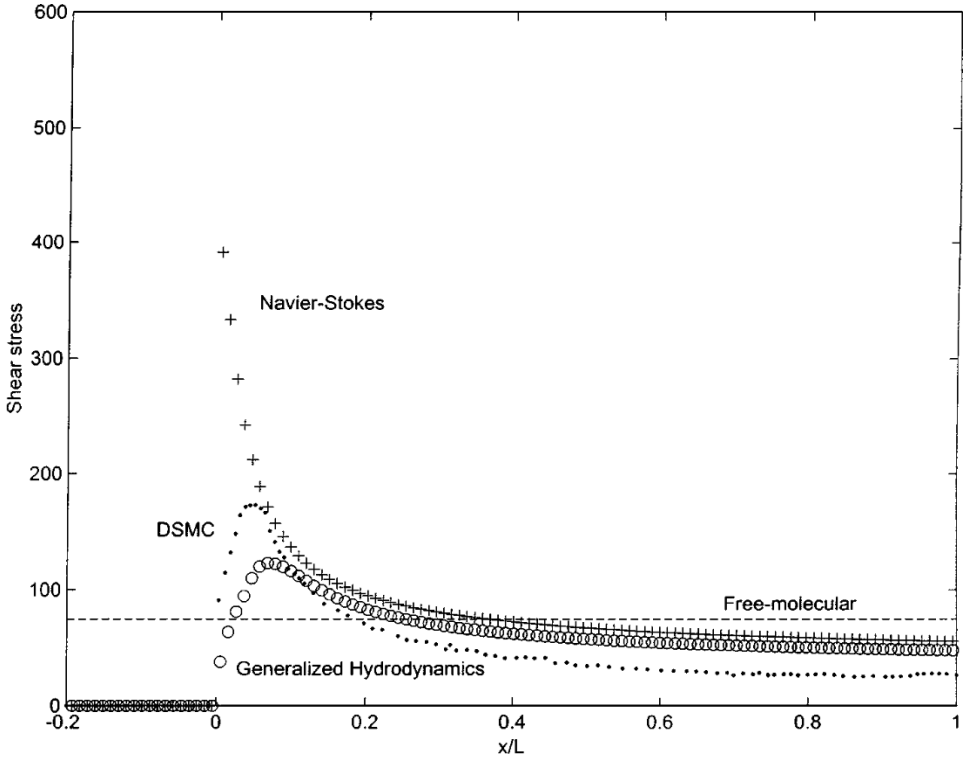
600
500
400
300
200
100
0
Shear stress
Navier-Stokes
DSMC
Free-molecular
Generalized Hydrodynamics
-0.2
0
0.2
0.4
0.6
0.8
1
x/L

Fig. 8